Forecasting Arctic sea ice drift: insights from two case studies

Ilona VALISUO,[1], and Steffen TIETSCHE[2]

[1]*Finnish Meteorological Institute, Helsinki, Finland*

[2]*European Centre for Medium Range Weather Forecasts, Bonn, Germany*

Correspondence: Ilona Välisuo <ilona.valisuo@fmi.fi>

ABSTRACT.

The two main large-scale features of Arctic sea ice drift are the Beaufort Gyre and the Transpolar Drift Stream. They exhibit strong intraseasonal and interannual variability. Winter 2016/2017 showed increased cyclone activity, leading to the collapse of the Beaufort Sea high and the reversal of the Beaufort Gyre. Winter 2020/2021 displayed decreased cyclone activity and intense anticyclonic ice transport in the Beaufort Gyre. Here we show that the ECMWF extended-range (46 days) retrospective forecasts were able to predict the ice motion during these cases. The initial contrasts in sea level pressure, surface winds and ice drift were well captured, and their temporal evolution – including the reversal of the usual drift direction – well reproduced by the forecasts initialized about a week before the event. Sea ice thickness in the forecast exhibited initial errors even greater than one meter that persisted throughout the forecast and negatively affected the ice speed forecast. Despite these shortcomings, the dynamic forecast outperformed the persistence and climatology forecast and represented the observed relation between surface winds and ice drift well. The benefit of dynamic forecasts is especially clear in cases that differ from climatology, like the one we focus on.

https://doi.org/10.1017/aog.2024.48 Published online by Cambridge University Press

INTRODUCTION

The ice drift redistributes ice inside the Arctic Ocean and exports ice from the Arctic Ocean. Ice motion can clear some areas from ice and create thicker ice in other places. Wintertime ice motion preconditions the upcoming melt season (Babb and others, 2019). Ice transport determines where the ice finally melts. Melting ice affects the local sea salinity and temperature and further the ocean currents. Accurate forecasts of sea ice drift in weekly scale are thus important when aiming for longer predictions of the Arctic sea ice and ocean.

Ice motion is a complex problem that depends on atmospheric and oceanic forcing, as well as sea ice properties. In the momentum equation of sea ice, the main drivers of the ice drift are winds, ocean currents and internal stresses, when the ice in not in free drift. Ice strength, which can be approximated with concentration and thickness, defines how the ice responds to the winds and currents. Minor contributors are the Coriolis effect and the sea surface tilt (Leppäranta, 2009). The two main large-scale features of Arctic Ocean sea ice motion are the Beaufort Gyre (BG) and the Transpolar Drift Stream (TDS) (Colony and Thorndike, 1984) (Fig.1). The BG is usually anticyclonic and transports multiyear ice from the Canadian Basin towards the Siberian Shelf. The TDS is directed from the Siberian Seas across the Arctic Ocean towards the Fram Strait. The TDS is an essential contributor to the ice transport away from the Arctic. It carries ice to the Fram Strait, the main route for ice export. About 14% to 15% of total Arctic Sea ice volume is exported every year, and the Fram Strait is the main export route of sea ice (Spreen and others, 2020; Babb and others, 2023). BG and TDS are quasi-permanent features but exhibit large variability in ice flow intensity and direction. There is an increasing trend in ice drift speed, which has been linked to changes in atmospheric pressure patterns (Kwok and others, 2013), and changes in ice strength rather than increased wind speed (Olason and Notz, 2014).

The predictability of sea ice conditions in sub-seasonal to seasonal timescales originates from the persistence or advection of sea-ice anomalies and ice interactions with the ocean and the atmosphere (Guemas and others, 2016). The initial ice thickness is crucial for ice concentration and thickness predictions (e.g. Guemas and others (2016); Chevallier and others (2019)). Currently, the ice thickness predictions are afflicted by the lack of data assimilation (e.g. Xiu and others (2022)) and too modest spread of initial ice thickness (Tietsche and others, 2018). The predictability of sea ice drift has received less attention than ice concentration and thickness. However, Schweiger and Zhang (2015) demonstrate skill for real-world forecasts up to one week ahead, and Reifenberg and Goessling (2022) report in a multimodel study that

https://doi.org/10.1017/aog.2024.48 Published online by Cambridge University Press

the Eulerian ice velocity vectors reached the climatological saturation value in 2-3 weeks. There are also ongoing efforts to utilize sea ice drift forecasts from numerical weather prediction centers to support the planning and operations of Arctic expeditions, such as the SIDFEx project in support of the MOSAiC expedition (Ludwig and others, 2023).

Here, we present two forecast case studies (February-March 2017 and 2021) focusing on sea ice drift in sections in the TDS and in the BG under cyclonic and anticyclonic atmospheric large-scale circulation. We study the European Centre for Medium-Range Weather Forecasts's (ECMWF) extended range forecasts that cover a forecast period of 46 days. Comparing ice drift forecasts between two distinct cases and assessing their quality with respect to the observed outcomes allows insight into how well the forecasting system represents the physical processes that determine sea ice drift; any deficits diagnosed should be addressed in order to improve predictive skill. Furthermore, the direct quantification of forecast errors days to weeks ahead gives some indication of the overall level of skill that can be expected from these forecasts. The results presented here provide a reference for future weather and climate models to improve upon. Better forecasts of sea ice drift in the Arctic regions will directly benefit marine users, and are also important for an improved understanding of the changing climate of the Arctic regions in the 21st century.

The paper is structured as follows: the Introduction and subsections give an overview of the Arctic atmospheric circulation and present the atmospheric condition during the winters of our case studies. Data and methods -section presents the forecast and reference data, defines the periods of the case studies, and describes the transects that we use to address the large-scale sea ice circulation. In Results, we present the initial conditions of the forecast cases in terms of maps and forecast evolution in terms of time series. One subsection addresses the relationship between wind speed and ice drift speed. Finally, the paper ends with Summary and Conclusions.

Arctic winter circulation

The typical winter mean sea level pressure field in the polar and sub-polar regions of the Northern Hemisphere is characterized by low-pressure systems in the North Atlantic and North Pacific and high pressure over the continents, especially Siberia. The Pacific half of the Arctic (divided along longitude 90° E-90° W) is under a high-pressure ridge that connects the Siberian and the Yukon highs. Due to this ridge, the Beaufort Sea high does not appear as a clear closed anticyclone but is influenced by the Siberian and Alaskan high pressures. The Atlantic half of the Arctic is influenced by the Icelandic low, which extends

https://doi.org/10.1017/aog.2024.48 Published online by Cambridge University Press

Fig. 1. A schematic map showing the Beaufort Gyre and the Transpolar drift stream, and the locations of the transects used in this study.

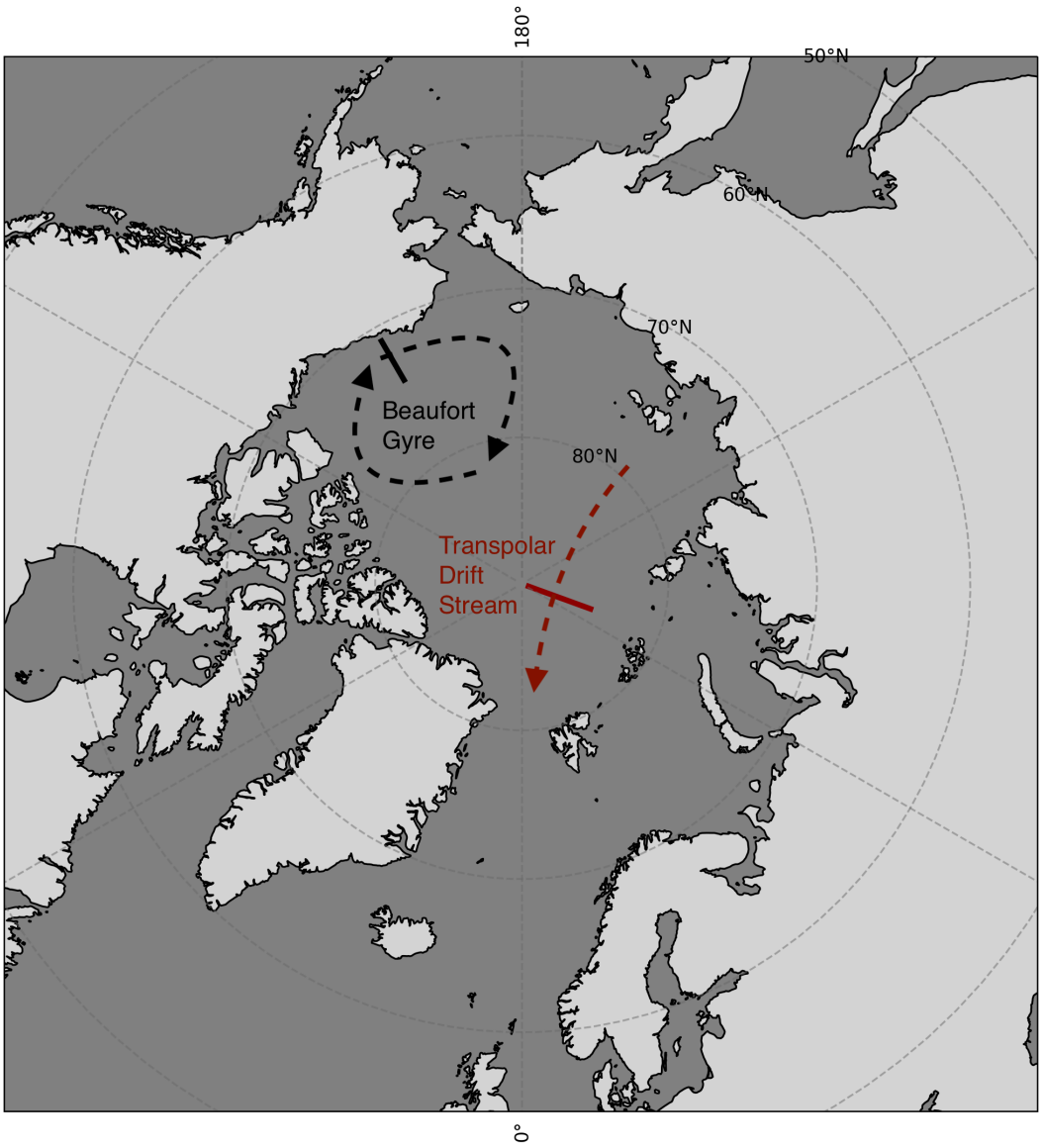

https://doi.org/10.1017/aog.2024.48 Published online by Cambridge University Press

northeast towards the Barents Sea. (Nygård and others, 2021; Serreze and Barrett, 2011)

In the stratosphere, a polar vortex forms around the pole in winter. While the stratosphere does not directly influence the surface weather, the stability of the polar vortex can affect the weather in the Arctic and mid-latitudes. For example, Sudden Stratospheric Warming (SSW) events, where the stratosphere warms abruptly, and the polar vortex gets unstable, tend to lead to warmer surface temperatures in the central Arctic in the weeks that follow the SSW (Baldwin and others, 2021). This was the case in winter 2021, which is one of the two cases studied here (Mallett and others, 2021).

Opposing circulation patterns in winters 2016/2017 and 2020/2021

Significant interannual variability is seen in the ice drift patterns, above all due to the variability in atmospheric conditions. During the past decade, winters 2016/2017 and 2020/2021 stand out with anomalous opposing atmospheric and sea ice circulation (Table 1).

Winter 2016/2017 was marked by record low Mean Sea Level Pressure (MSLP), which led to the reversal of the normally anticyclonic atmospheric and sea ice circulation in the Beaufort Sea region. This is sometimes referred to as a collapse of the Beaufort Sea high pressure. Moore and others (2018) provide a thorough analysis of the winter 2016/2017 circulation anomaly, which we summarise here. The negative MSLP anomaly occurred in January-March. It was caused by a sequence of low-pressure systems rather than one long-lived pressure pattern. The foundation for the anomaly was laid already in the previous autumn. Warm autumn of 2016 led to thin ice cover, which contributed to the formation of a thermal low pressure in the Barents Sea. The Barents low favored the propagation of Atlantic low pressures to the Arctic. In January-March, a sequence of low-pressure systems traveled from the North Atlantic to the Siberian coast in the Arctic Basin. This caused the collapse of the Beaufort Sea High and the reversal of Beaufort Gyre. The Transpolar Drift stream was less intense than usual and was at times directed back to the Arctic Basin rather than towards the Fram Strait. The whole season was warmer than average over almost the entire Arctic.

In winter 2020/2021, the MSLP averaged over the Arctic (north of 60° N) was at a record high, and surface winds and ice transport were anticyclonic. Winter 2020/2021 has been studied by Mallett and others (2021), to whom we refer in this paragraph. The average December-January-February (DJF) MSLP north of 60° N was the second highest since 1979. The Arctic Oscillation -index over DJF was the second most negative since 1979. The positive MSLP anomaly occurred especially in January-February, with a

https://doi.org/10.1017/aog.2024.48 Published online by Cambridge University Press

Table 1. Summary of winter conditions 2017 and 2021.

	Winter 2016-2017	Winter 2020-2021
Characteristics	Record low MSLP. The collapse of the Beaufort Gyre.	Record high MSLP. Strong ice export.
Timing	Jan-Mar 2017.	Jan-Feb. 2021 with a peak on 11th Feb.
Causes	Sequence of low-pressure systems.	Persistent high pressure.
References	Moore and others (2018)	Mallett and others (2021)

peak on the 11.02.2021. The anomaly was a long lasting circulation regime, unlike in 2017, when a series of disturbances caused the anomaly. In the first months of 2021, the Yukon and Siberian high pressures were weak, and the Arctic high pressure appeared as an almost closed anticyclone rather than the typical ridge that connects the Siberian high to the high pressure over North America. This anticyclone resembled the Beaufort Sea high but was shifted east and poleward. The high pressure anomaly extended towards the Atlantic, and made the Barents Sea low pressure weaker than usual. In the Pacific sector, the Aleutian low was deeper than average. The anomaly was caused, at least partly, by a SSW that began on the 05.01.2021, degraded the polar low, and was reflected by higher-than-average MSLP in the Arctic (Mallett and others, 2021). In this winter 2020/2021, the Beaufort Gyre was strong, and so redistribution of multiyear ice and ice export via Transpolar drift stream were important.

Both anomalies were strong in February. In 2021 the Pan-Arctic MSLP was highest on the 11.02.2021 (Mallett and others, 2021), and in 2017 anomalous conditions occurred between January and March (Moore and others, 2018). We analysed atmospheric and sea ice conditions in February, and that allowed us to compare two different cases that took place in the same season. We focus on analysing the sea ice drift and thickness. We study the forecasts initialized on the 07.02.2017 and 07.02.2021.

DATA AND METHODS

Forecasts and reference data

We use extended-range retrospective forecasts from the European Center for Medium-Range Weather Forecasts (ECMWF), see Vitart and others (2017). The forecasts are produced using the IFS-NEMO-model with the LIM2 sea ice component. LIM2 is a dynamic-thermodynamic sea ice model with viscous-plastic rheology and a single thickness category (Fichefet and Maqueda, 1997). The coupled model takes into account the atmospheric and oceanic forcing and sea ice properties that all affect the ice motion.

https://doi.org/10.1017/aog.2024.48 Published online by Cambridge University Press

The IFS model version is 47R3. The forecast has eleven ensemble members: one control member and ten perturbed. The forecast length is 46 days. We compute daily means from 6-hourly instantaneous values. The horizontal resolution is about 15 km for the ocean and sea ice in the Arctic and about 35 km for the atmosphere. We retrieved data at a coarser $0.5^\circ \times 0.5^\circ$ horizontal resolution (equivalent to about 55km).

Verification of atmospheric forecasts is done against the ERA5 reanalysis (Hersbach and others, 2020). Its grid resolution is 31km. The data are available at an hourly temporal resolution (except for uncertainties, which are available at a 3h output frequency). ERA5 uses the 4D-Var assimilation scheme. In terms of the ocean, it assimilates sea surface temperatures (SST) and sea ice concentrations. ERA5 is fully described in Hersbach and others (2020).

For verification of sea ice drift forecasts, we use observations from the Polar Pathfinder dataset, which contains daily sea ice motion vectors on a 25 km EASE-Grid (Version 4). Polar Pathfinder merges data from satellite sensors, the International Arctic Buoy Program, and the NCEP/NCAR Reanalysis to generate the ice motion estimates. The Arctic data is available at a 25km$\times$25km National Snow and Ice Data Center's Equal-Area Scalable Earth-grid (NSIDC EASE-Grid North, EPSG:3408) (Tschudi and others, 2019). We use the Polar Pathfinder data to compute climatology and persistence forecasts. The climatology forecast is computed from the observed mean value on the same calendar date across the reference period 2000 - 2022. The persistence forecast is constructed by persisting the observed value on the initial day throughout the forecast.

We verify forecasts of sea ice thickness against observations from CryoSat2-SMOS (CS2-SMOS), a satellite-based sea ice thickness product. CS2-SMOS combines CryoSat-2 satellite altimeter observations and Soil Moisture and Ocean Salinity (SMOS) satellite radiometer retrievals of the sea ice thickness (Ricker and others, 2017). The advantage of the merged product is good performance for both thin and thick ice, as well as good spatio-temporal coverage.

Case studies

We compare two forecasts during anomalous cyclonic and anticyclonic circulation over the Arctic Ocean in early 2017 and 2021, as described in the Opposing Circulation Patterns –section. We select forecasts that are initialized on the 07.02.2017 and 07.02.2021. The selected forecasts cover the most intensive anomalies, as the anomalies occurred in January-March 2017 and peaked on the 11.02.2021 (Mallett and others, 2021; Moore and others, 2018). We study the forecast initial conditions of sea ice concentration, thickness,

https://doi.org/10.1017/aog.2024.48 Published online by Cambridge University Press

motion, and atmospheric conditions in both forecasts. Further, we study the forecast evolution at selected transects in the Beaufort Gyre (at 210° E) and in the Central Arctic at the Transpolar Drift Stream (at 70° E). Forecast conditions at the transects allow us to analyze how the most critical Arctic sea ice drift patterns are reproduced in the forecasts. This provides insight into how well the forecasts represent the processes determining the sea ice drift and which level of forecast skill can be expected.

Transects

We define two transects: one in the Beaufort Sea, which we call the BG–transect, and one in the TDS in the central Arctic. The aim is to quantify the ice drift speed across the transects, and compare the conditions between the two locations and two cases. Each transect provides a snapshot of the drift speed in the drift pattern. We interpret these simple local measures of ice drift speed together with the large scale atmospheric circulation, thus being able to understand the behaviour of the entire drift pattern.

The TDS–transect is defined along longitude 70° E and covers latitudes 85°–89.5° N. The transect contains nine grid points as we use the 0.5° ×0.5° forecast output, and its length is about 500m. The exact location of the TDS varies, but our transect captures the most important features of the drift. The BG–transect is located at the southern Beaufort Sea at 210° E and 71-74° N. It contains six grid points of the forecast data and it is about 330m long. The location of the BG–transect is selected following Mallett and others (2021). The transects are marked in Figures 1-4.

RESULTS

Forecast initial conditions

We compare forecasts that are initialized on the 07.02.2017 and 07.02.2021. The forecasts cover the most intensive pressure anomalies that occurred around February in both cases (Opposing Circulation patterns –Section). Maps in Figures 2-4 show the average over the first day of the forecasts. The difference in MSLP (Fig. 2) is evident: in 2017, a low pressure pattern covers the North-Atlantic, Greenland, Canadian Archipelago, and Central Arctic. The air pressure was lower than average in the corresponding regions (Fig. 1 in the supplement). The Eurasian continent is under a high pressure, and the sea level pressure was higher that average over the Eurasian continent (Fig. 1 in the supplement). In 2021, Central Arctic and Greenland are under a strong high pressure system. At the same time, an intensive low pressure is seen over Russia. A positive pressure anomaly covered the whole Arctic, while the Siberian high pressure

https://doi.org/10.1017/aog.2024.48 Published online by Cambridge University Press

was weaker than usual (Fig. 1 in the supplement). The maps present the condition of one day but coincide with the overall winter anomalies of the selected years. Near-surface temperature (Fig. 2) is higher in 2017 than in 2021 all over the Arctic Ocean and surrounding continents.

As we focus on winter conditions, the difference in sea ice concentration between the two years is not prominent in the Central Arctic, but differences are seen at the ice edge (Fig 3). Most of the Arctic Ocean is fully ice-covered. In the Labrador Sea, the sea ice edge extends further south in 2017 than in 2021. This seems to be caused by the intensive Icelandic low, which created northerly winds and ice transport in the Labrador Sea region (Fig. 4). The Barents Sea was mostly ice-free in 2017. The higher sea ice concentration in the Barents Sea in 2021 is linked to the low pressure over Russia, which created northerly flow in the Barents Sea and transported ice further south.

Sea ice is thinner in the beginning of February 2017 than in 2021 (Fig. 3), especially in the Beaufort Sea. Thinner ice in the Beaufort Sea is likely a result of the weak Beaufort Gyre and reduced eastward transport of multiyear ice, as well as warmer air temperatures in 2017 than in 2021. The anomalies of sea ice thickness are shown in the supplementary Fig. 2, which shows that ice in the Beaufort Sea region was thinner that average in 2017 and thicker than average in 2021.

Ice drift speed (Fig. 4, panels c and d) reflects the general circulation pattern (see Fig. 2 for MSLP, and Fig. 4 for 10m wind speed), and sea ice concentration and thickness. According to the forecast initial conditions, the ice drift speed is less than 0.15 m/s, or 13 km/day, in the Central Arctic. At the margins, the ice speed reaches 0.9 m/s, or 78km/day. The speed is fastest where the ice is thin, or the concentration is low. This is seen at the margins of the sea ice, but also in the Central Arctic, for example, in 2017 north of the New Siberian Islands, where the area of faster ice speed coincides with thinner ice. There is no clear cyclonic circulation at the Beaufort Sea in either case. This might be because of the absence of a clear Beaufort Sea High and the fact that the Beaufort Gyre is an average circulation pattern, whereas our maps present daily snapshots.

All in all, the initial conditions on the 07.02.2017 and 07.02.2021 reflect well the negative MSLP anomaly in 2017 and the positive anomaly in 2021. The sea ice thickness is also different between the two cases, generally thicker in 2021, which is important for the forecast evolution.

https://doi.org/10.1017/aog.2024.48 Published online by Cambridge University Press

Fig. 2. Mean sea level pressure and 2 m temperature on the first day of the 07.02.2017 and 07.02.2021 forecasts. The black line shows the location of the Beaufort Gyre –transect, and the red line shows the Transpolar Drift Stream transect.

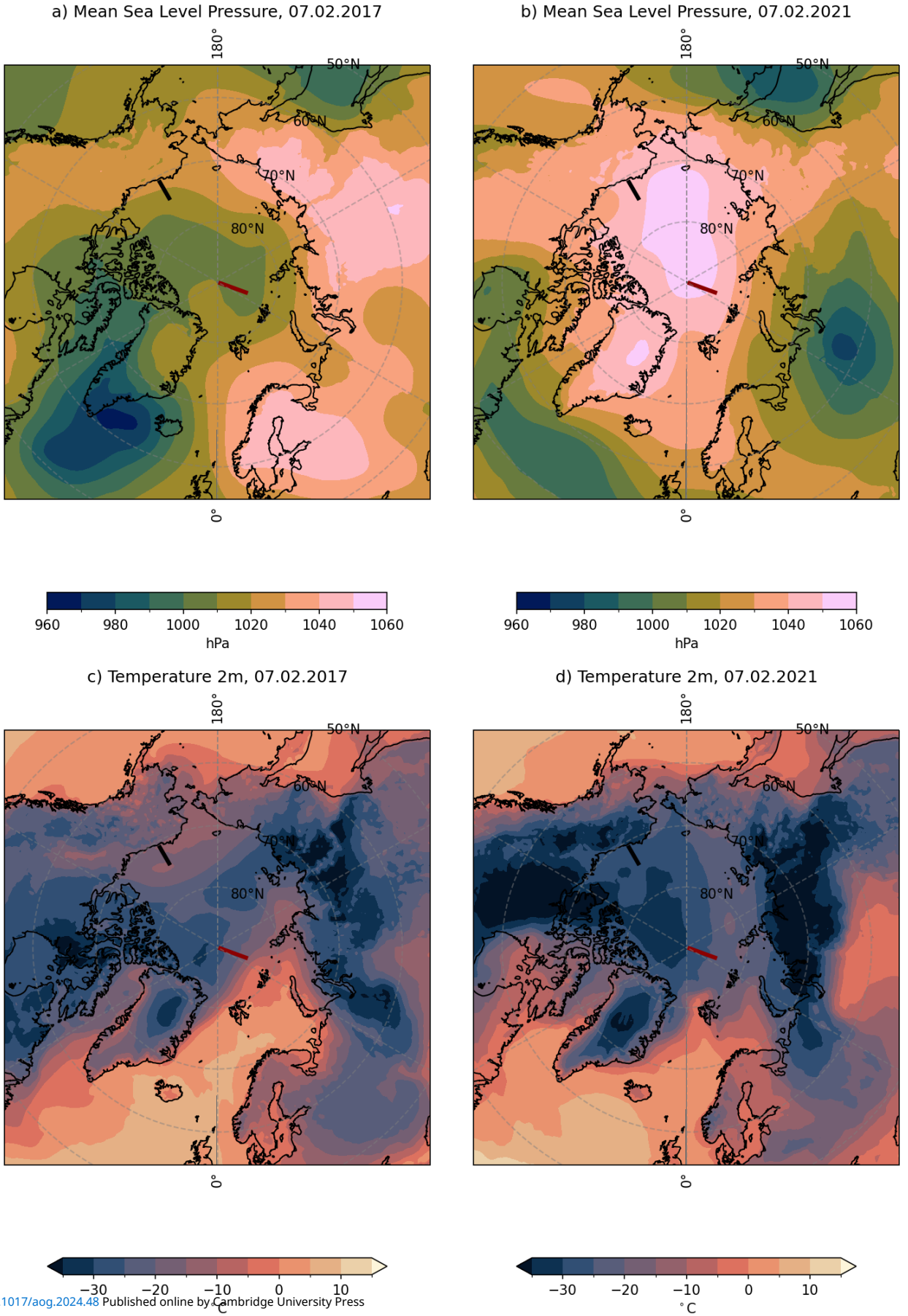

https://doi.org/10.1017/aog.2024.48 Published online by Cambridge University Press

Fig. 3. Sea ice concentration and sea ice thickness on the first day of the 07.02.2017 and 07.02.2021 forecasts. The black line shows the location of the Beaufort Gyre transect, and the red line shows the Transpolar Drift Stream transect.

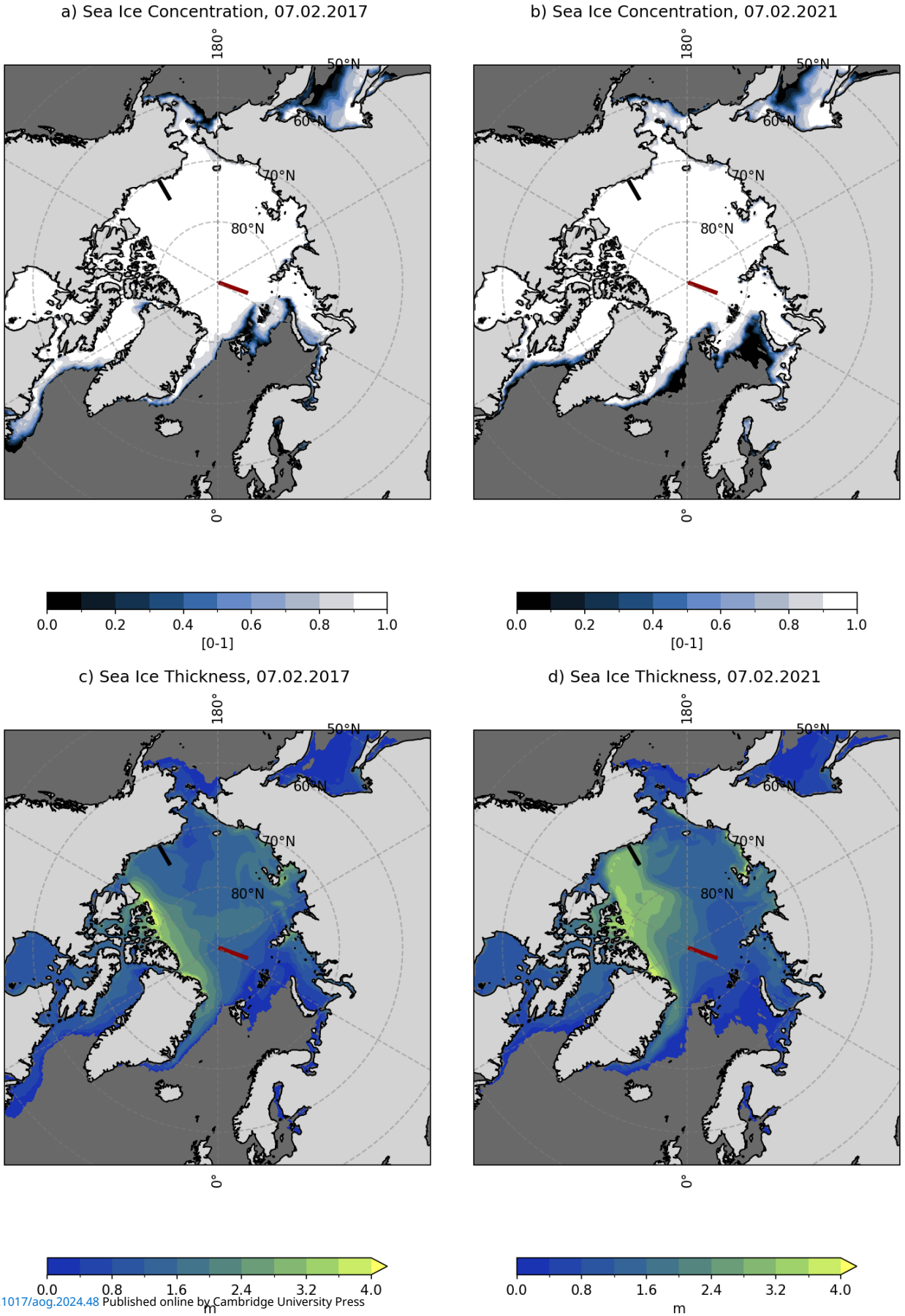

https://doi.org/10.1017/aog.2024.48 Published online by Cambridge University Press

Fig. 4. Wind at 10m height and ice drift on the first day of the 07.02.2017 and 07.02.2021 forecasts. The black line shows the location of the Beaufort Gyre transect, and the red line shows the Transpolar Drift Stream transect.

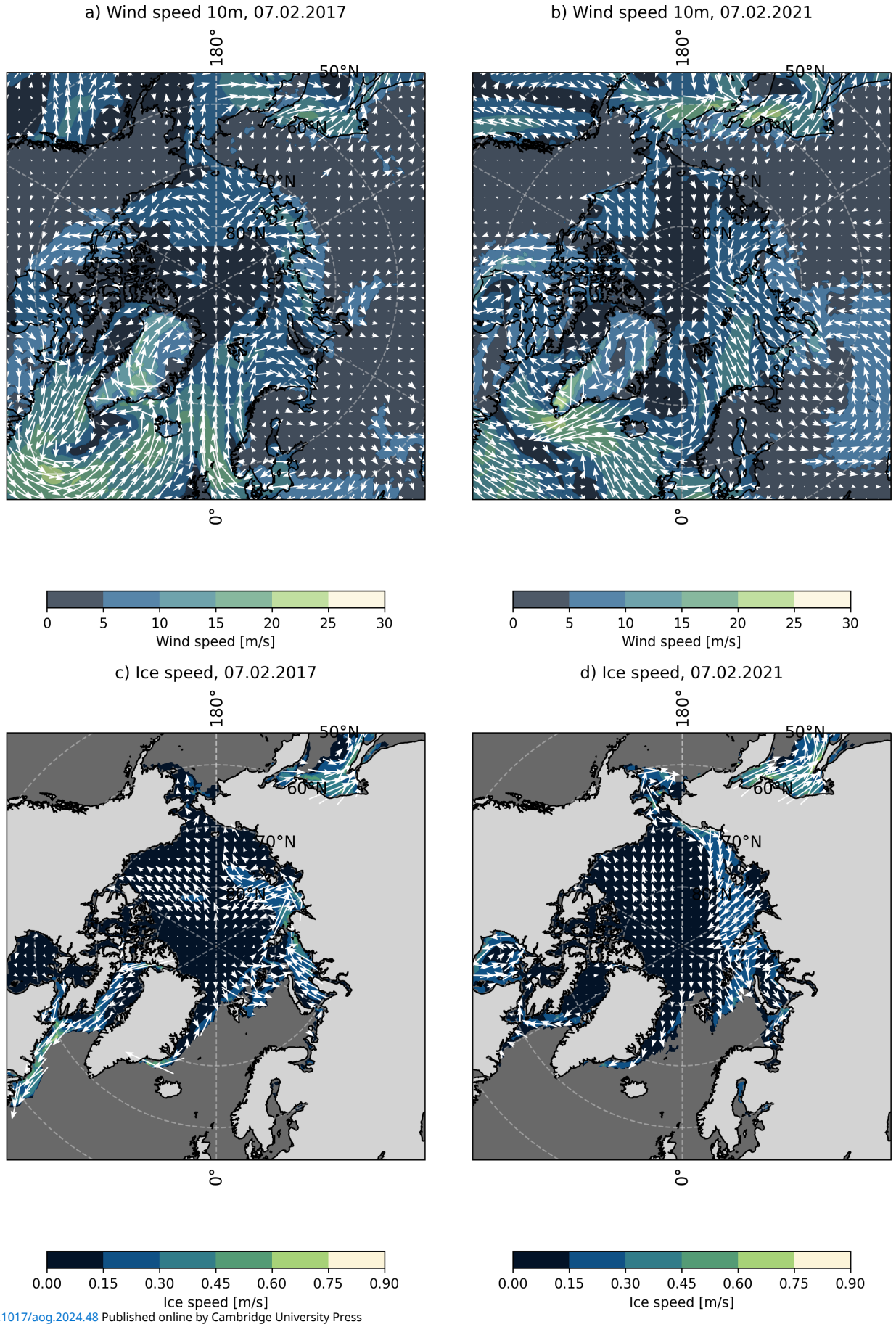

https://doi.org/10.1017/aog.2024.48 Published online by Cambridge University Press

Forecast evolution

We have defined two transects: one for the BG, and one for the TDS. We discuss forecasts of atmospheric variables (mean sea level pressure, temperature at 2m height, wind speed normal to the transect at 10 m height) and sea ice variables (sea ice concentration, sea ice thickness, and drift speed normal to the transect) at the transect locations to compare the two locations and two cases. We evaluate the quality of the forecasts by comparing their evolution against reanalysis and observations. In general, the cases are clearly distinct from each other, and locations have their own characteristics. We anticipate that the beginning of the forecast is in agreement with the observations, but the predictability can be considerably weakened after about two weeks of forecast time. However, for a well-calibrated forecast ensemble, we should expect the observations to lie within the ensemble range throughout the forecast, if the initial conditions and the forecast model are of high quality.

The time series of the sea level pressure reveals the cyclonic conditions in 2017 (Fig. 5, panels a and b), and anticyclonic conditions in 2021 (Fig. 5, panels a and b). In 2017, the initial sea level pressure (Fig. 6) was approximately 1030 hPa and decreased to approximately 990 hPa during the first week of the forecast in both locations. In 2021, the starting level was around 1050 hPa at BG and TDS (Fig. 6). In 2021, the peak value for sea level pressure is forecast on the 07.02.2021 at TDS and 09.02.2021 at BG. These dates are close to the pan-Arctic maximum of the sea level pressure, which occurred on the 11.02.2021 according to Mallett and others (2021). The ensemble mean predicts the evolution seen in ERA5 quite well until a lead time of about three weeks, around the 01.03. in both cases. We also note that at the beginning of the forecast, the sea level pressure increases and decreases simultaneously between the two locations, indicating that both places are affected by the same large-scale pressure patterns.

The time series of air temperature at 2 m height shows the relatively warm conditions in 2017 and cold conditions in 2021 at the beginning of the forecast (Fig. 5, panels c and d, and Fig. 6 panels c and d). The forecast 2 m temperature does not match ERA5 as well as in the case of MSLP. ERA5 2 m temperature is mostly within the ensemble spread but sometimes hits and exceeds the limits of the ensemble. We note that ERA5 data indicates a strong warm advection from the Atlantic to the TDS–transect from 15.02.2021 to 01.03.2021. One ensemble member of the forecast actually predicts this strong increase in 2 m temperature, but the ensemble mean indicates about 20° C colder temperatures. At the BG–transect, the timing of 2 m temperature anomalies is very different between the forecast and ERA5 between 15.02.2017-01.03.2017, suggesting that 2 m temperature forecast skill for this case is lost after about a week. Unlike for MSLP,

https://doi.org/10.1017/aog.2024.48 Published online by Cambridge University Press

there is no clear simultaneous increase or decrease in temperature between the locations. The temperature evolution thus seems more local than the MSLP evolution.

Near-surface wind speed is related to the sea level pressure gradient. Figures 5 and 6 show the average u-component (zonal) of the 10m wind at BG and TDS. As the transects are defined along the longitudes, the zonal component is normal to the transect. Positive zonal wind indicates eastward flow. Hence, at BG, the positive zonal wind speed is from the the Chukchi Sea towards the Canadian basin. At TDS, the positive zonal wind is from the Atlantic towards the Siberian Seas. The average flow directions are westward, i.e., from the Canadian Basin towards the Chukchi Sea at BG, and from the Siberian Seas towards the Atlantic. Therefore, a negative zonal wind speed is typical at BG and TDS, and the positive values indicate anomalies. ERA5 shows positive zonal wind speed from around 07.02.2017 to 17.02.2017 at BG and TDS, reflecting the anomalous cyclonic circulation of the case. The forecast captures the westward (positive zonal wind speed) flow at the beginning of the forecast but falls eastward (negative zonal wind speed) faster than ERA5. In 2021, the beginning of the forecast is characterized by strong westward winds at BG and TDS. The forecast is in good agreement with ERA5 for at least the first week of the forecast. At TDS, from 15.02.2021 to 01.03.2021, the ERA5 wind speed follows the maximum limit of the ensemble spread (given by any ensemble member, not necessarily one single member), as it did in the case of 2 m temperature. This indicates a strong advection of warm air from the Atlantic towards the central Arctic. Interestingly, the event cannot be noticed in the MSLP time series (Fig. 6, panel a). The variability of the forecast near-surface wind speed is smaller than in ERA5, which might, in part, be attributable to the small ensemble size of just 11 members.

The sea ice thickness forecasts are notably different from the CS2-SMOS ice thickness (Fig. 5, panels g and h, and Fig. 6 panels g and h). The average ice thickness of the forecasts does not compare well with CS2-SMOS-thickness, and neither do the forecasts capture the observed temporal evolution of the ice thickness. At the TDS–transect, the forecast ice thickness is consistently underestimated compared to CS2-SMOS. In 2021, the forecast thickness evolution failed to capture the relatively abrupt increase in ice thickness that occurred roughly between 15.02.2021 and 22.02.2021, according to the CS2-SMOS data. This sudden increase in ice thickness coincides with the easterly winds seen in the ERA5 data. However, neither the forecast nor the Polar Pathfinder drift speed increased during that time. At the BG–transect, we pay attention to the large difference, about 1.5 m, in the forecast ice thickness between the two cases. CS2-SMOS-thickness suggests that the forecast model overestimated the ice thickness in

https://doi.org/10.1017/aog.2024.48 Published online by Cambridge University Press

Fig. 5. Time series of forecast and reference data at the Transpolar Drift Stream– and Beaufort Gyre–transects during the 07.02.2017 -case. Figure shows the mean sea level pressure (MSLP), the 2 meter tempearture (T2m), the 10 meter wind speed (u10m), and the sea ice thickness (SIT). Reference data is ERA5 for atmospheric variables and CS2-SMOS for ice thickness. The legend is shown on the right-hand side panels but also applies to the left-hand side.

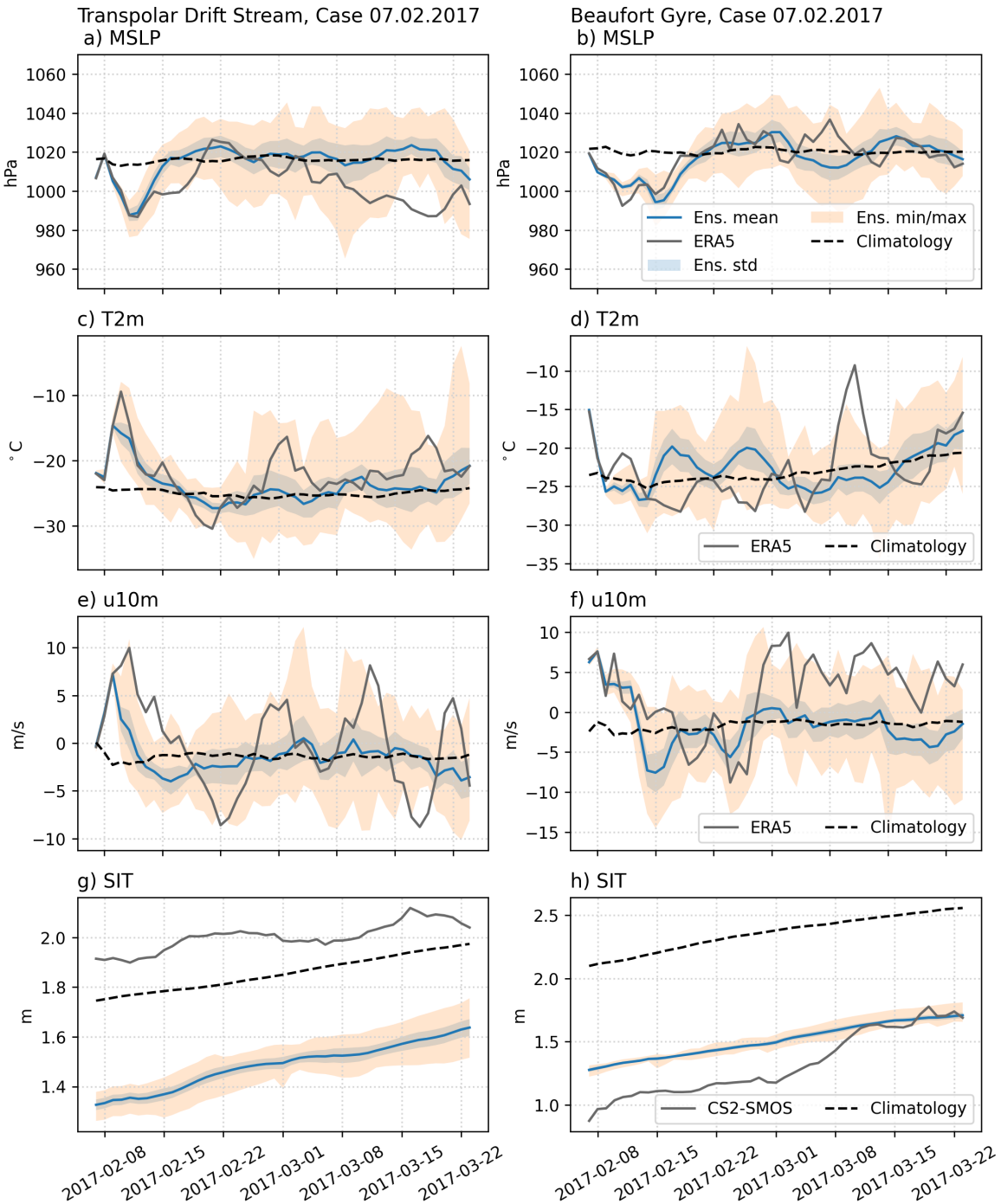

https://doi.org/10.1017/aog.2024.48 Published online by Cambridge University Press

Fig. 6. Time series of forecast and reference data at the Transpolar Drift Stream– and Beaufort Gyre–transects during the 07.02.2021 -case.Figure shows the mean sea level pressure (MSLP), the 2 meter tempearture (T2m), the 10 meter wind speed (u10m), and the sea ice thickness (SIT). Reference data is ERA5 for atmospheric variables and CS2-SMOS for ice thickness. The legend is shown on the right-hand side panels but also applies to the left-hand side.

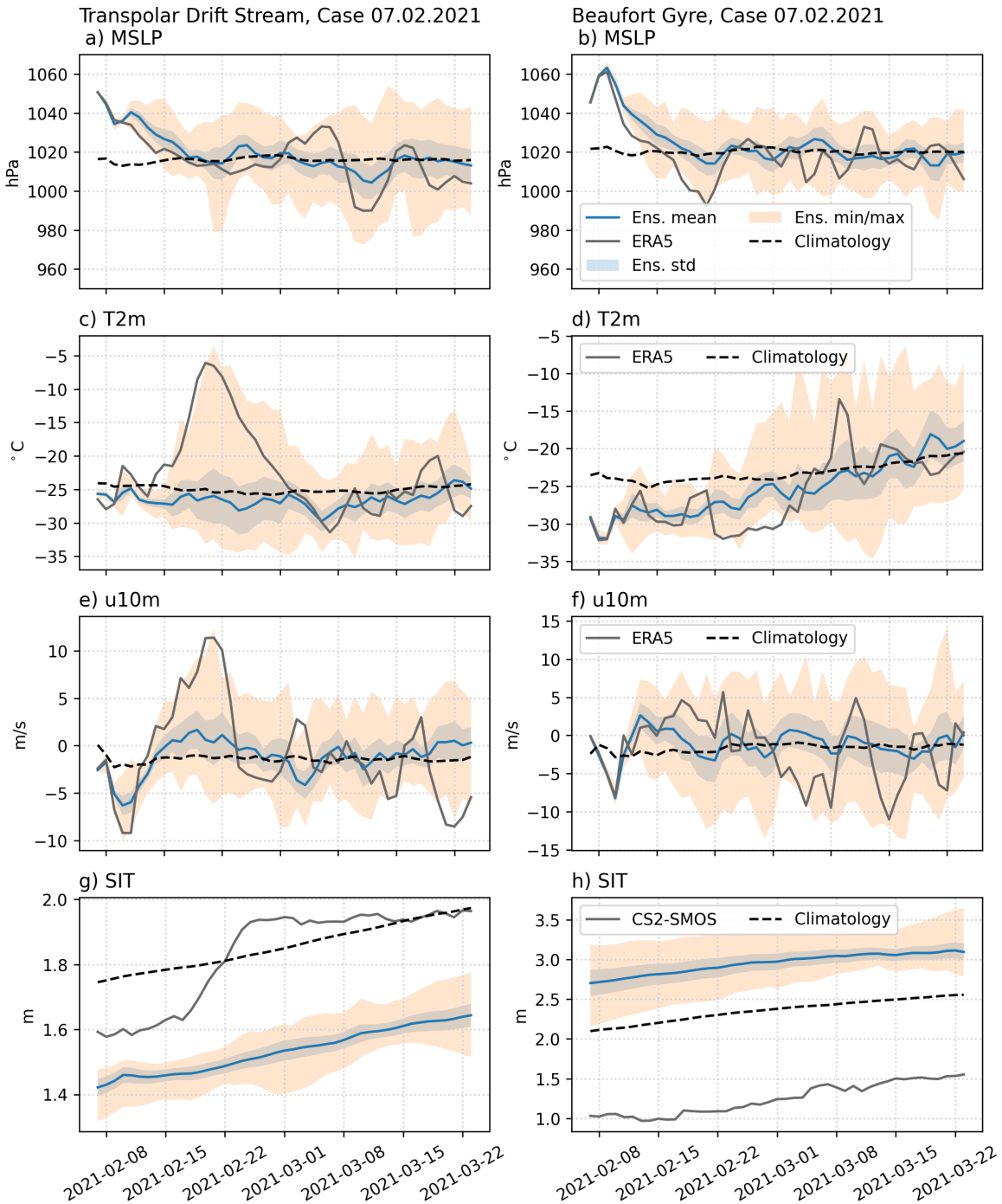

https://doi.org/10.1017/aog.2024.48 Published online by Cambridge University Press

Fig. 7. Time series of the sea ice drift speed in forecasts and reference data. The blue line shows the ensemble mean, the blue shading the ensemble standard deviation, and the orange shading the ensemble minimum and maximum values. The solid grey line shows the Polar Pathfinder reference data, the long dashes show the climatology forecast, and the fine dashes show the persistence forecast.

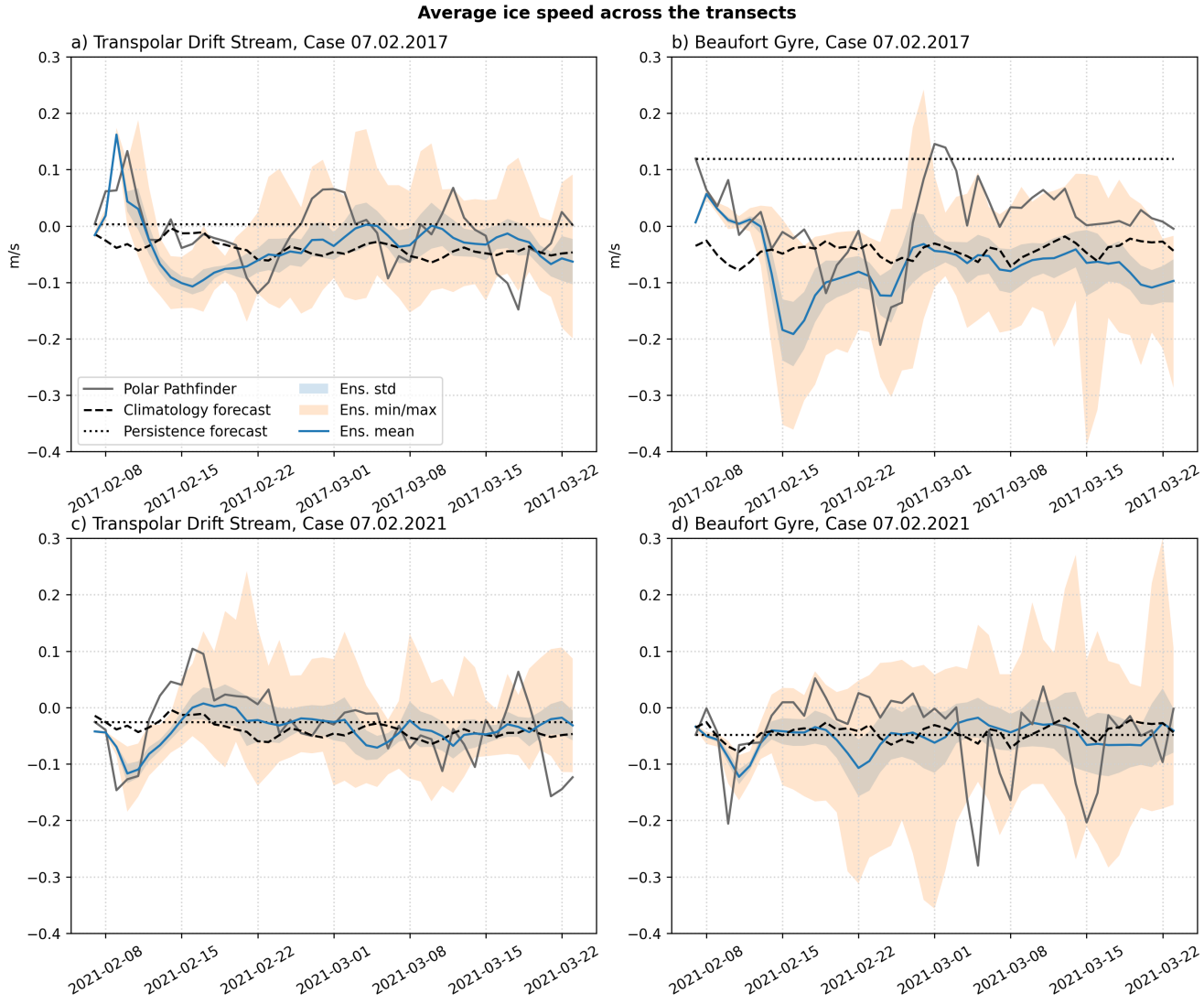

https://doi.org/10.1017/aog.2024.48 Published online by Cambridge University Press

2021. The forecast ice was thicker than observed at the beginning of the forecast in 2017, but by the end of the forecast, the observed ice thickness increased to the same values as the forecast. The described discrepancies between forecast and observed sea ice thickness at the transects reflect current shortcomings of the forecast models, such as lack of thickness assimilation (Xiu and others, 2022) and underspread of initial ice thickness (Tietsche and others, 2018).

The ice drift speed across the transect is shown in Figure 7. As in the case of wind speed, the u-component (zonal) of ice speed describes the ice flow normal to the transect, and negative values indicate the typical flow direction. For the drift speed across the section, we also provide two simple statistical reference forecasts: climatology and persistence. Both are simple to construct from observations and can serve as a benchmark for the dynamical forecasts. The climatology forecast is computed from the observed mean value on the same calendar date across the reference period 2000 - 2022. The persistence forecast is constructed by persisting the observed value on the initial day throughout the forecast.

As we can see from Fig. 7, the initial conditions of the two cases are clearly different, but the differences fade after the first 1-2 weeks of the forecast. At the TDS section (Fig. 7, panels a and c), the typical flow direction is westward (negative u), which means ice transport towards the Atlantic. The climatology forecast indicates westward flow in both cases. At TDS, the persistence forecast, i.e. assuming that the drift speed stays the same as on day one of the forecast, is close to the climatology. The dynamic forecast captures the difference between the cases. The year 2017 shows an untypical eastward ice motion at the TDS section at the beginning of the forecast, which can be interpreted as a temporary reversal of the Transpolar Drift Stream. The reference data indicates eastward flow, or very weak flow, for almost two weeks while the forecast shifts to westward in less than a week. This is likely the cause for the intense build-up of ice thickness in the CS2-SMOS observations, which is absent in the forecasts. Later, the forecast ensemble spread grows, and the flow across the transect settles to slightly westward (negative values), which is the typical flow direction of the Transpolar Drift. In 2021, the flow behavior was the opposite: strongly negative in the first days of the forecast, followed by just about positive ensemble mean zonal drift at days 10-14 of the forecast, and after that, settling to the climatological westward flow. It is worth noting that ERA5 showed a strong eastward wind at TDS in 15.02.2021-22.02.2021, but this is not seen in the Polar Pathfinder data: ice flow barely turns eastward.

Ice velocity across the BG–transect is shown in Figure 7, panels b and d. In 2017, we see the reversal of the Beaufort Gyre as positive zonal drift, which is far from the forecast climatology at the beginning of the

https://doi.org/10.1017/aog.2024.48 Published online by Cambridge University Press

Fig. 8. Ice drift speed forecast error and root mean square error (RMSE) across the transects. The mean is calculate over years the 2000 - 2022.

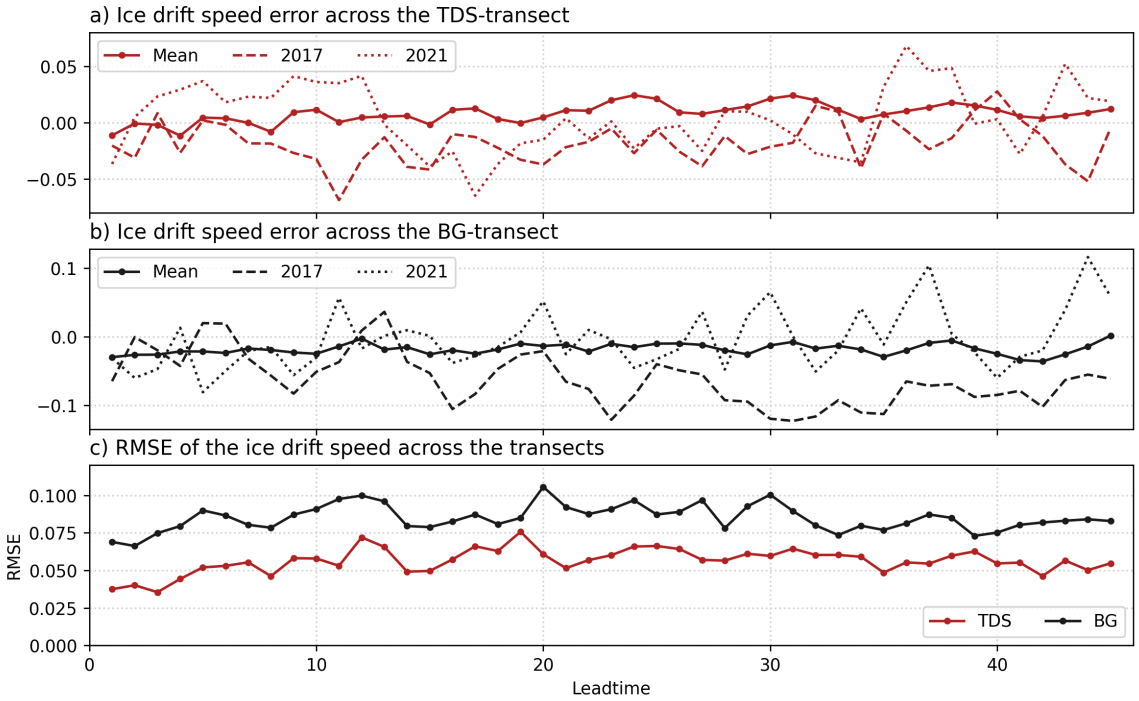

forecast. In the forecast, the positive values are followed by drift speeds of c. -0.2 m/s around 15.2.2017, while the Polar Pathfinder drift speed is close to zero during these dates. At the end of February and beginning of March, the Polar Pathfinder data shows another reversal of the Beaufort gyre. The forecast ensemble mean does not reach a positive value, but some ensemble members also capture the possibility for reversed BG. In the 2021 case, the forecast shows strong westward ice drift during the first week of the forecast, then settling for weaker yet eastward flow. This behaviour is consistent with the Polar Pathfinder data. In both cases, the Polar Pathfinder data show more frequently positive ice velocities across the transect, i.e. momentary reversals of the Beaufort Gyre. The forecast follows the climatological anticyclonic circulation more closely, as indicated by the negative drift speed across the BG–transect.

Figure 8 puts the performance of the forecasts for the two cases we study here into the context of the average forecast performance over many cases. We computed forecast errors for all forecasts started on 31 January, 07 February and 14 February for all years between 2002 and 2021 (60 forecasts). By comparing Figure 8a,b with Fig 8c we see that – although the 2017 and 2021 cases were very unusual in many respects

https://doi.org/10.1017/aog.2024.48 Published online by Cambridge University Press

– the ice drift forecast errors through both transects were within the expected errors (about 0.05 m/s for the BG–transect and about 0.08 m/s for the TDS–transect). The average forecast errors during the first week of the forecast are surprisingly large. When plotting errors against ORAS5, the ocean reanalysis product that the forecasts are initialized from, we confirm the expected behaviour of small initial errors that somewhat saturate after about 2-3 weeks (not shown). This indicates that, importantly, the uncertainty of the sea ice analysis plays a significant role for the forecast performance in the first 2-3 weeks.

Wind speed and ice drift relationship

Figure 9 shows scatter plots of ice drift speed across the transect (usi) and wind speed across the transect (u10m) from the forecasts. Ice and wind speed are correlated in all the cases, with correlation coefficients ranging from 0.66 (BG–transect, 2021) to 0.82 (TDS–transect, 2017). The ice speed and wind speed are more variable at the BG–transect than TDS–transect, especially because of more frequent negative drift speed i.e. anticyclonic circulation. The corresponding plots based on Polar Pathfinder ice speed and ERA5 wind speed are shown in Figure 10. The correlation coefficient ranges from 0.76 (TDS–transect, 2021) to 0.90 (BG–transect, 2017), thus higher than for the forecasts. The forecast data suggest higher maximum ice and wind speeds than the reference data from Polar Pathfinder and ERA5. However, only a small number of forecast ensemble members suggest these higher speeds.

The strong correlation between ice drift speed and 10 m wind speed is expected, and reflects the dominating impact of surface winds on the ice drift. It is worth noting that we have compared the the zonal component of the wind speed and drift speed. As there direction of the wind driven ice drift is deviated to the right for the wind speed direction, we expect higher correlation between the absolute wind speed and drift speed. The most plausible explanation for the remaining scatter is differences in the internal ice forces and oceanic drag. The oceanic drag is not independent of the ice thickness. Dynamic ice growth and formation of pressure ridges increase the drag at the ice-ocean interface. Furthermore, we note the impact of sea ice thickness on the correlation between ice drift and 10 m wind speed: the strong overestimation of ice thickness in the forecast in the BG in 2021 (3 m instead of 1 m) is associated with a markedly lower correlation in the forecast (0.66) than in the observations (0.78). This is expected because internal ice forces are stronger in thicker ice. Overall, the forecast clearly represents the observed correlation between surface wind and sea ice drift.

Similar scatter plots were created for the ice speed–ice thickness relationship (not shown). According

https://doi.org/10.1017/aog.2024.48 Published online by Cambridge University Press

to these plots, the forecast ice speed and thickness are not correlated, nor is the thin ice moving faster than thick ice. Correlation coefficients between the forecasted ice speed and ice thickness at TDS–transect were -0.06 and -0.07 (cases 2017 and 2021, respectively); and at BG–transect -0.11 and 0.09 (cases 2017 and 2021, respectively). Generally, thicker ice is advected across the transects later in the forecast, except for the BG2021 case, where the thickening is not so clear (Fig. 6). The reference data indicates a similar ice speed–thickness relationship to the forecasts: no clear dependence of ice speed on ice thickness, but increasing ice thickness from the beginning of February until late March.

Climatological studies have shown that the ice drift speed in the Arctic has increased, and the driver of the speed up is not increased wind speed but decreased ice concentration and thickness (e.g. Kwok and others (2013), Olason and Notz (2014)). A modeling study by Li and others (2024) finds also that the changes in ice speed are linked to the changes in ice thickness distribution. Our case studies show a strong relationship between 10 m wind speed and ice drift speed but no correlation between ice thickness and ice drift speed.

https://doi.org/10.1017/aog.2024.48 Published online by Cambridge University Press

Fig. 9. Scatter plots of ice speed and wind speed across the transects. The plots are based on all ensemble members of the forecasts, and the colorscale shows the forecast time step from the 7th of February to the 23rd of March. The black line shows a linear fit to all data points.

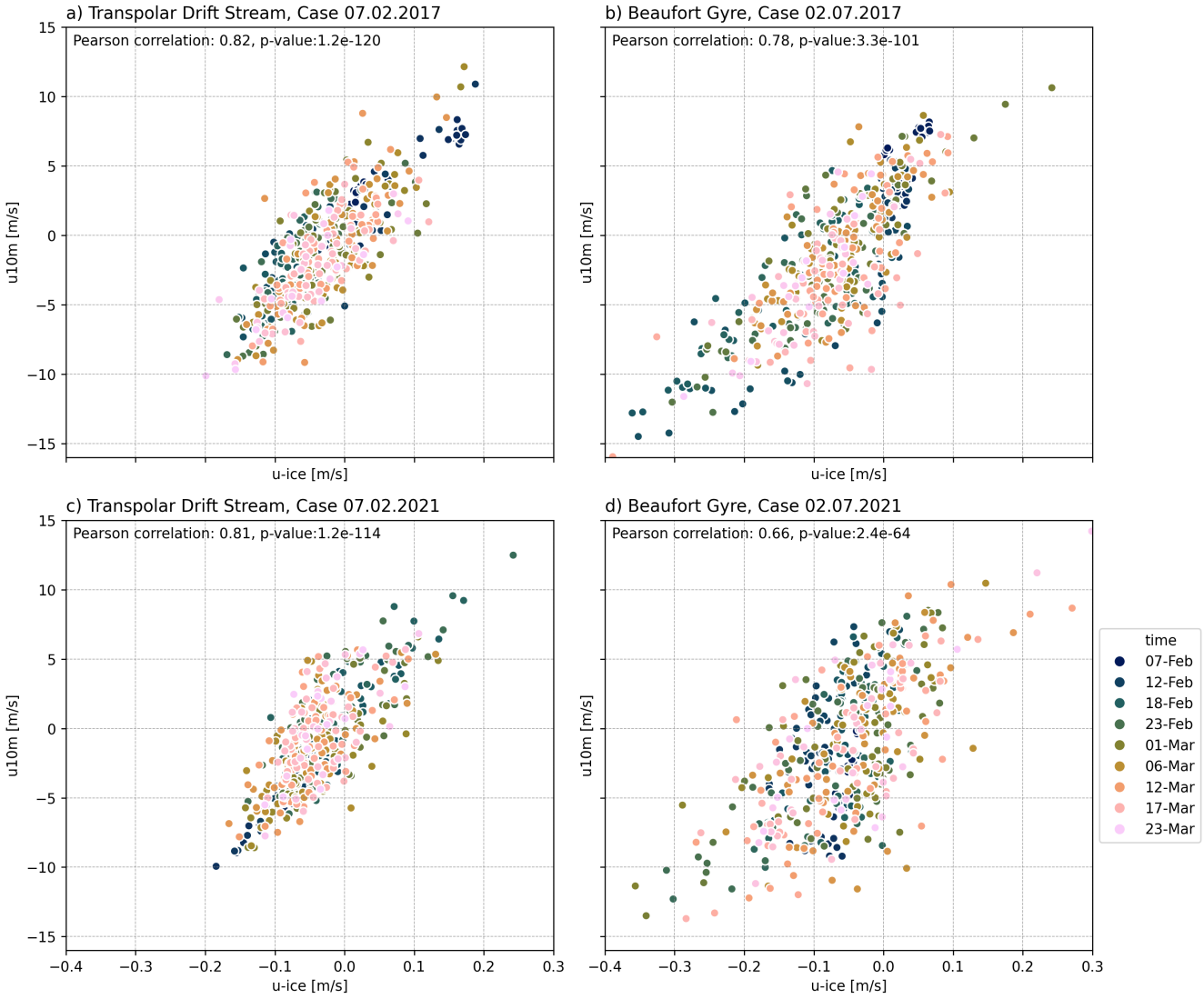

https://doi.org/10.1017/aog.2024.48 Published online by Cambridge University Press

Fig. 10. Scatter plots of reference ice speed (Polar Pathfinder) and wind speed (ERA5) across the transects. The color scale shows the forecast time step from the 7th of February to the 23rd of March.

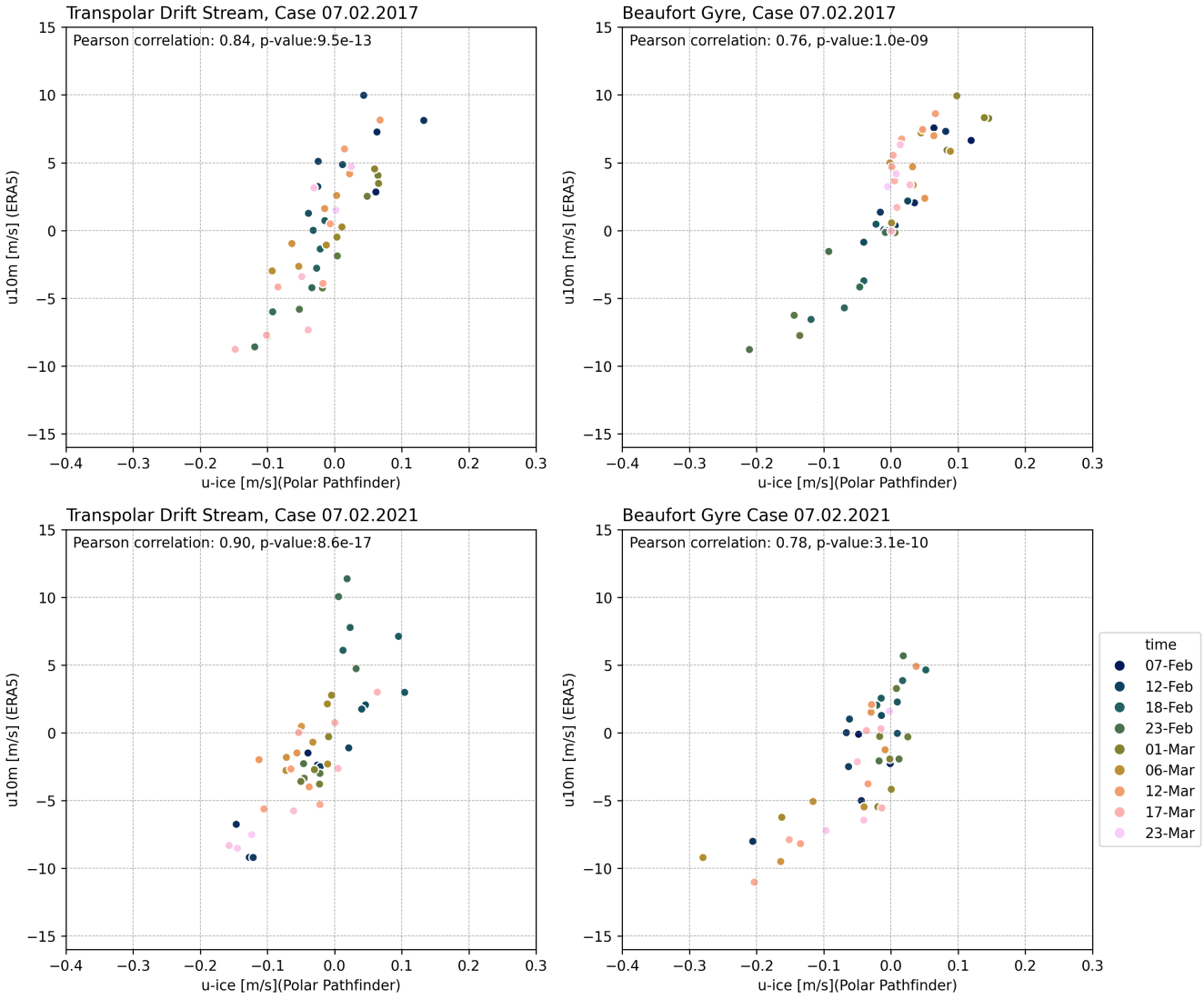

https://doi.org/10.1017/aog.2024.48 Published online by Cambridge University Press

SUMMARY AND CONCLUSIONS

We present two case studies with opposing initial MSLP patterns in the Arctic. According to previous studies, the selected cases represent extreme anomalies in the MSLP (Mallett and others, 2021). We focus on the ice drift in the Beaufort Gyre and the Transpolar drift stream. These case studies enlighten the ice drift forecastt̀s behaviour under contrasting atmospheric forcing and help in evaluating the usefulness of the drift forecast under unusual conditions.

The ECMWF's extended-range forecasts captured the atmospheric conditions in these two cases of exceptionally cyclonic and anticyclonic circulation mostly well. The forecasted large-scale circulation patterns (MSLP) of winters 2017 and 2021 compare well with the ERA5 –data. The variability of the near-surface wind speed forecast appears underestimated compared to ERA5. It is worth noting that the forecast ensemble is only 11 members, and the wind speed forecast might profit from a larger ensemble. One ensemble member captures a prominent warm air advection event, visible in the 2 m temperature and 10 m zonal wind, at the TDS in 2021.

Compared to CS2-SMOS observations, the forecast overestimated the thickness at TDS– and underestimated it at the BG–transect. Already, the initial state of the ice thickness is erroneous, which is a common problem as sea ice thickness is not assimilated in forecast models (Xiu and others, 2022). The initial ice thickness affects the thermodynamic growth of ice and the dynamics of ice. In our case studies, the forecast fails to capture the rapid increase of sea ice thickness at the TDS –transect in 2021 and at the BG –transect in 2017. The ice thickness increase at TDS in 2021 coincides with the observed warm advection and westerly winds. Further, the large bias in sea ice thickness potentially affects the ice drift speed.

The dynamical ice drift forecasts outperform the climatology and persistence forecasts in both cases and locations. Climatology and persistence forecasts do not capture the drift variations that are present in the forecast and observations. The benefit of dynamic forecasts is especially clear in cases that differ from climatology, like the ones we focus on.

Trying to link the ice drift and ice thickness evolution, we pay attention to the observed rapid increase in the ice thickness at the TDS in 2021. This increasing ice thickness is preceded by eastward ice speed in the Polar Pathfinder–data, strong westerly winds, and warm temperature according to ERA5. The westerly winds possibly blocked the TDS momentarily, allowing the accumulation and advective thickening of sea ice in the location. At least one forecast member captured these features, but none of the forecast

https://doi.org/10.1017/aog.2024.48 Published online by Cambridge University Press

members indicated a clear increase in the ice thickness.

The forecast model produces a reasonable relationship between the near-surface wind speed and ice drift speed. The relationship is less well represented in cases where the erroneous ice thickness affects the mobility of the ice. At the BG–transect in 2021, the forecast overestimated the ice thickness, which made the ice less responsive to the wind forcing and leads to lower correlation than observed. The comparison of the two cases highlights that the variability of the near-surface wind speed is essential for forecasting the ice speed correctly, as expected. The ice thickness was not related to the drift speed. This suggests that either the internal ice stresses were of minor importance in these two cases or the forecast model was unable to reproduce the relationship between drift speed and ice thickness.

In summary, our study presents two contrasting case studies focusing on ice drift behavior in the Arctic. These cases, characterized by extreme anomalies in the MSLP, shed light on the effectiveness of ice drift forecasts under varying atmospheric conditions. The ECMWF extended range forecasts generally align well with observed atmospheric patterns, although the near-surface wind speed variability seems underestimated when compared to ERA5. Notably, the initial state of ice thickness introduces errors, impacting both thermodynamic growth and ice dynamics. Despite these challenges, dynamic ice drift forecasts outperform climatology and persistence models, emphasizing their value in anomalous and quickly changing circulation regimes. The strengths and weaknesses of the dynamic ice drift forecasts discussed here can inform future developments of improved forecasting systems and contribute to a better understanding of sea ice drift processes in a quickly changing Arctic Ocean.

ACKNOWLEDGEMENTS

This study was supported by the Research Council of Finland through the project "Understanding the sub-seasonal to seasonal predictability of Arctic sea ice.", agreement number 339409. The production of the merged CryoSat-SMOS sea ice thickness data was funded by the ESA project SMOS & CryoSat-2 Sea Ice Data Product Processing and Dissemination Service, and data from 01.01.2011 to 31.12.2022 were obtained from AWI. The forecasts and ERA5 -products are provided by the ECMWF, for which we are thankful. We thank also the NASA National Snow and Ice Data Center Distributed Active Archive Center for making the Polar Pathfinder dataset available.

REFERENCES

Babb DG, Landy JC, Barber DG and Galley RJ (2019) Winter Sea Ice Export From the Beaufort Sea as a Preconditioning Mechanism for Enhanced Summer Melt: A Case Study of 2016. *Journal of Geophysical Research: Oceans*, **124**(9), 6575–6600, ISSN 2169-9291 (doi: 10.1029/2019JC015053), _eprint: https://onlinelibrary.wiley.com/doi/pdf/10.1029/2019JC015053

Babb DG, Kirillov S, Howell SEL, Landy JC, Glissernaar I, J S, Brady M and Ehn J (2023) The complete annual record of sea ice volume export through fram strait as observed by satellite from 2010-2022. *ESS Open Archive* (doi: 10.22541/essoar.170110665.58564319/v1)

Baldwin MP, Ayarzagüena B, Birner T, Butchart N, Butler AH, Charlton-Perez AJ, Domeisen DIV, Garfinkel CI, Garny H, Gerber EP, Hegglin MI, Langematz U and Pedatella NM (2021) Sudden stratospheric warmings. *Reviews of Geophysics*, **59**(1), e2020RG000708 (doi: https://doi.org/10.1029/2020RG000708), e2020RG000708 10.1029/2020RG000708

Chevallier M, Massonnet F, Goessling H, Guémas V and Jung T (2019) Chapter 10 - The Role of Sea Ice in Subseasonal Predictability. In AW Robertson and F Vitart (eds.), *Sub-Seasonal to Seasonal Prediction*, 201–221, Elsevier, ISBN 978-0-12-811714-9 (doi: https://doi.org/10.1016/B978-0-12-811714-9.00010-3)

Colony R and Thorndike AS (1984) An estimate of the mean field of Arctic sea ice motion. *Journal of Geophysical Research: Oceans*, **89**(C6), 10623–10629, ISSN 2156-2202 (doi: 10.1029/JC089iC06p10623), _eprint: https://onlinelibrary.wiley.com/doi/pdf/10.1029/JC089iC06p10623

Fichefet T and Maqueda MAM (1997) Sensitivity of a global sea ice model to the treatment of ice thermodynamics and dynamics. *Journal of Geophysical Research*, **102**(C6), 12609–12646, ISSN 0148-0227 (doi: 10.1029/97JC00480)

Guemas V, Blanchard-Wrigglesworth E, Chevallier M, Day JJ, Déqué M, Doblas-Reyes FJ, Fukar NS, Germe A, Hawkins E, Keeley S, Koenigk T, Salas y Mélia D and Tietsche S (2016) A review on Arctic sea-ice predictability and prediction on seasonal to decadal time-scales. *Quarterly Journal of the Royal Meteorological Society*, **142**(695), 546–561, ISSN 00359009 (doi: 10.1002/qj.2401)

Hersbach H, Bell B, Berrisford P, Hirahara S, Horányi A, Muñoz-Sabater J, Nicolas J, Peubey C, Radu R, Schepers D, Simmons A, Soci C, Abdalla S, Abellan X, Balsamo G, Bechtold P, Biavati G, Bidlot J, Bonavita M, De Chiara G, Dahlgren P, Dee D, Diamantakis M, Dragani R, Flemming J, Forbes R, Fuentes M, Geer A, Haimberger L, Healy S, Hogan RJ, Hólm E, Janisková M, Keeley S, Laloyaux P, Lopez P, Lupu C, Radnoti G, de Rosnay P, Rozum I, Vamborg F, Villaume S and Thépaut JN (2020) The ERA5 global reanalysis. *Quarterly Journal of the Royal Meteorological Society*, **146**(730), 1999–2049, ISSN 1477-870X (doi: 10.1002/qj.3803), _eprint: https://onlinelibrary.wiley.com/doi/pdf/10.1002/qj.3803

https://doi.org/10.1017/aog.2024.48 Published online by Cambridge University Press

Kwok R, Spreen G and Pang S (2013) Arctic sea ice circulation and drift speed: Decadal trends and ocean currents. *Journal of Geophysical Research: Oceans*, **118**(5), 2408–2425, ISSN 2169-9291 (doi: 10.1002/jgrc.20191), _eprint: https://onlinelibrary.wiley.com/doi/pdf/10.1002/jgrc.20191

Leppäranta M (2009) Sea Ice Dynamics. In JH Steele (ed.), *Encyclopedia of Ocean Sciences (Second Edition)*, 159–169, Academic Press, Oxford, second edition edition, ISBN 978-0-12-374473-9 (doi: https://doi.org/10.1016/B978-012374473-9.00640-8)

Li M, Liang X, Liu N, Zhao F and Tian Z (2024) Responses of the arctic sea ice drift to general warming and intraseasonal oscillation in the local atmosphere. *Climate Dynamics* (doi: https://doi.org/10.1007/s00382-024-07395-9)

Ludwig V, Goessling H and Team S (2023) The Sea Ice Drift Forecast Experiment (SIDFEx): Introduction and Applications (doi: 10.5281/zenodo.7874854)

Mallett RDC, Stroeve JC, Cornish SB, Crawford AD, Lukovich JV, Serreze MC, Barrett AP, Meier WN, Heorton HDBS and Tsamados M (2021) Record winter winds in 2020/21 drove exceptional Arctic sea ice transport. *Communications Earth & Environment*, **2**(1), 1–6, ISSN 2662-4435 (doi: 10.1038/s43247-021-00221-8), number: 1 Publisher: Nature Publishing Group

Moore GWK, Schweiger A, Zhang J and Steele M (2018) Collapse of the 2017 Winter Beaufort High: A Response to Thinning Sea Ice? *Geophysical Research Letters*, **45**(6), 2860–2869, ISSN 1944-8007 (doi: 10.1002/2017GL076446), _eprint: https://onlinelibrary.wiley.com/doi/pdf/10.1002/2017GL076446

Nygård T, Tjernström M and Naakka T (2021) Winter thermodynamic vertical structure in the arctic atmosphere linked to large-scale circulation. *Weather and Climate Dynamics*, **2**(4), 1263–1282 (doi: 10.5194/wcd-2-1263-2021)

Olason E and Notz D (2014) Drivers of variability in Arctic sea-ice drift speed. *Journal of Geophysical Research: Oceans*, **119**(9), 5755–5775, ISSN 2169-9291 (doi: 10.1002/2014JC009897), _eprint: https://onlinelibrary.wiley.com/doi/pdf/10.1002/2014JC009897

Reifenberg SF and Goessling HF (2022) Predictability of Arctic sea ice drift in coupled climate models. *The Cryosphere*, **16**(7), 2927–2946, ISSN 1994-0416 (doi: 10.5194/tc-16-2927-2022), publisher: Copernicus GmbH

Ricker R, Hendricks S, Kaleschke L, Tian-Kunze X, King J and Haas C (2017) A weekly arctic sea-ice thickness data record from merged cryosat-2 and smos satellite data. *The Cryosphere*, **11**(4), 1607–1623 (doi: 10.5194/tc-11-1607-2017)

Schweiger AJ and Zhang J (2015) Accuracy of short-term sea ice drift forecasts using a coupled ice-ocean model. *Journal of Geophysical Research: Oceans*, **120**(12), 7827–7841, ISSN 2169-9291 (doi: 10.1002/2015JC011273), _eprint: https://onlinelibrary.wiley.com/doi/pdf/10.1002/2015JC011273

Serreze MC and Barrett AP (2011) Characteristics of the Beaufort Sea High. *Journal of Climate*, **24**(1), 159–182, ISSN 0894-8755, 1520-0442 (doi: 10.1175/2010JCLI3636.1), publisher: American Meteorological Society Section: Journal of Climate

Spreen G, de Steur L, Divine D, Gerland S, Hansen E and Kwok R (2020) Arctic Sea Ice Volume Export Through Fram Strait From 1992 to 2014. *Journal of Geophysical Research: Oceans*, **125**(6), e2019JC016039, ISSN 2169-9291 (doi: 10.1029/2019JC016039), _eprint: https://onlinelibrary.wiley.com/doi/pdf/10.1029/2019JC016039

Tietsche S, Alonso-Balmaseda M, Rosnay P, Zuo H, Tian-Kunze X and Kaleschke L (2018) Thin Arctic sea ice in L-band observations and an ocean reanalysis. *The Cryosphere*, **12**(6), 2051–2072, ISSN 1994-0416 (doi: 10.5194/tc-12-2051-2018), publisher: Copernicus GmbH

Tschudi M, Meier WN, Stewart JS, Fowler C and Maslanik J (2019) Polar pathfinder daily 25 km ease-grid sea ice motion vectors, version 4 (doi: 10.5067/INAWUWO7QH7B)

Vitart F, Ardilouze C, Bonet A, Brookshaw A, Chen M, Codorean C, Déqué M, Ferranti L, Fucile E, Fuentes M, Hendon H, Hodgson J, Kang HS, Kumar A, Lin H, Liu G, Liu X, Malguzzi P, Mallas I, Manoussakis M, Mastrangelo D, MacLachlan C, McLean P, Minami A, Mladek R, Nakazawa T, Najm S, Nie Y, Rixen M, Robertson AW, Ruti P, Sun C, Takaya Y, Tolstykh M, Venuti F, Waliser D, Woolnough S, Wu T, Won DJ, Xiao H, Zaripov R and Zhang L (2017) The Subseasonal to Seasonal (S2S) Prediction Project Database. *Bulletin of the American Meteorological Society*, **98**(1), 163–173, ISSN 0003-0007, 1520-0477 (doi: 10.1175/BAMS-D-16-0017.1), publisher: American Meteorological Society Section: Bulletin of the American Meteorological Society

Xiu Y, Luo H, Yang Q, Tietsche S, Day J and Chen D (2022) The challenge of arctic sea ice thickness prediction by ecmwf on subseasonal time scales. *Geophysical Research Letters*, **49**(8), e2021GL097476 (doi: https://doi.org/10.1029/2021GL097476), e2021GL097476 2021GL097476